AIAA JOURNAL
Vol. 39, No. 4, April 2001

Roughness-Induced Attachment-Line Transition on a Swept Cylinder in Supersonic Flow

Colin P. Coleman*
NASA Ames Research Center, Moffett Field, California 94035-1000
and
D. I. A. Poll†
Cranfield University, Cranfield, Bedfordshire, England MK43 OAL, United Kingdom

Experiments were conducted on a 76-deg swept cylinder to establish the conditions for transition onset at the attachment line with and without surface roughness in a low-disturbance (quiet), Mach 1.6 airflow. Local flow parameters were estimated from surface pressure measurements, and hot wires and schlieren photography were used to determine the state of the boundary layer. It was found that, for a near-adiabatic wall condition and a smooth surface, the attachment-line boundary layer remained laminar up to the highest Reynolds number ($\bar{R}$ of 790) attainable in the tunnel. Transition under the influence of trip wires was found to depend on wind-tunnel disturbance levels, and the onset conditions have been established.

Nomenclature

a	=	speed of sound, $a = \sqrt{(\gamma RT)}$
C_p	=	coefficient of pressure, $(p - p_\infty)/0.5\gamma M_\infty^2 p_\infty$
D	=	diameter of circular cylinder
k	=	diameter of trip wire
M	=	Mach number
p	=	pressure
p_{rms}	=	root mean square of the total pressure
p_{total}	=	total pressure
Q_∞	=	freestream velocity
R	=	gas constant for air, 287 J/kg K
$\bar{R}$	=	attachment-line Reynolds number, $V_e\eta_e/\nu_e$
$\bar{R}_*$	=	transformed attachment-line Reynolds number, $V_e\eta_*/\nu_*$
Re_k	=	trip wire Reynolds number (based on boundary-layer edge conditions), $V_e k/\nu_e$
Re_∞	=	freestream unit Reynolds number, Q_∞/ν_∞
r	=	recovery factor, $(T_r - T)/(T_0 - T)$
s	=	distance from trip wire (or cylinder tip if no trip wire present) to hot-wire position, measured along attachment line
T	=	temperature
T_*	=	Poll's reference temperature, $T_e + 0.1(T_w - T_e) + 0.6(T_r - T_e)$ (Ref. 17)
U, V, W	=	velocity components in x, y, and z directions, respectively
x	=	chordwise direction (normal to attachment line)
y	=	spanwise direction (along attachment line)
z	=	normal direction (normal to cylinder surface)
γ	=	ratio of specific heats of air
δ	=	boundary-layer thickness at $V/V_e = 0.99$
η_e	=	viscous length scale, $\nu_e/(\mathrm{d}U_e/\mathrm{d}x)_{x=0}]^{1/2}$
η_*	=	transformed viscous length scale, $\nu_*/(\mathrm{d}U_e/\mathrm{d}x)_{x=0}]^{1/2}$
θ	=	angle measured from attachment line in x direction
Λ_m	=	model sweep angle
Λ_s	=	shock wave angle
ν	=	kinematic viscosity

Subscripts

A	=	conditions at the edge of the attachment-line boundary layer
e	=	conditions at the edge of the boundary layer
r	=	conditions based on the recovery temperature, T_r
w	=	surface of cylinder (wall conditions)
0	=	stagnation conditions
∞	=	freestream conditions
$*$	=	conditions based on the reference temperature, T_*

Received 20 June 1999; revision received 25 September 2000; accepted for publication 27 September 2000.

*Research Scientist, Department of Fluid Mechanics Laboratories, M.S. 260-1. Member AIAA.
†Head, College of Aeronautics. Associate Fellow AIAA.

Introduction

THE incomplete understanding of the attachment-line (Fig. 1) and crossflow transition processes is one of the fundamental obstacles to the development of an economically viable, supersonic, laminar flow aircraft. In the presence of small surface roughness, the flow along an attachment line may become turbulent at the lowest Reynolds number of all of the transition mechanisms that can be active on a swept wing. Moreover, because the resulting turbulence propagates in both the spanwise and chordwise directions, when the attachment line becomes turbulent, the flow over the whole wing, both upper and lower surfaces, will also become turbulent. Therefore, attachment-line transition is an important consideration in the design process.

Improvement in understanding can only come by the analysis of data obtained from carefully designed and carefully conducted experiments, preferably ones in which engineering issues and questions of fundamental physics can be addressed at the same time. In the case of the attachment-line flow, experiments conducted on swept cylinders are valuable because it is possible to generate very large values of the local boundary-layer Reynolds number at the appropriate values of the Mach number at the edge of the layer and the wall temperature. Hence, on relatively small wind-tunnel models, data that are directly applicable to flight can be obtained, and the physics of transition can be studied at flight scale.

To date, no theoretical model for the stability of a compressible attachment-line flow has been fully validated. The main reason for this is the very limited amount of accurate, experimental data currently available. Although transition has been observed for smooth and tripped configurations over a wide range of freestream Reynolds numbers and Mach numbers,[1–8] there have been no measurements in unstable viscous layers at, or near, an attachment line in low supersonic Mach number flow over a near adiabatic wall. Therefore, experiments[9,10] were conducted to establish the behavior of

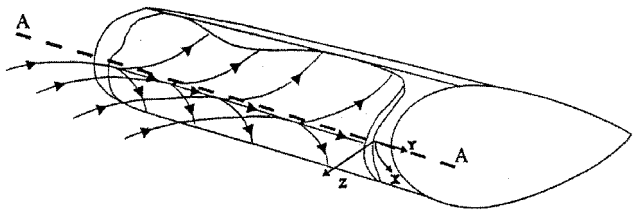

Fig. 1 Attachment line (line A–A) boundary layer formed on the leading edge of a swept cylinder.

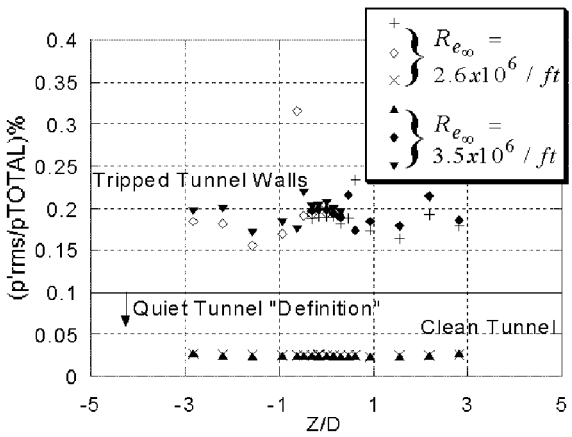

Fig. 2 Pressure fluctuations across the center of the test section, 1.0 in. downstream of the nozzle exit with and without tripped tunnel walls; 250 Hz–100 kHz range.

the attachment-line transition process in a low-disturbance (quiet) Mach number 1.6 flow.

Description of Wind Tunnel and Models

Tests were carried out in the Mach 1.6 Quiet Wind Tunnel at the Fluid Mechanics Laboratory, NASA Ames Research Center. This facility, described in detail in Refs. 9, 11, and 12, was designed to produce laminar flow on the tunnel walls to reduce the radiated disturbance environment in the test section. This produces a novel, low freestream turbulence and low-noise-level flow for unit Reynolds number ranging from 2.4×10^6/ft to 3.6×10^6/ft. Figure 2 shows the test section pressure fluctuations ($p_{\text{rms}}/p_{\text{total}}$) at a location 1 in. downstream of the nozzle exit, as determined by the measurement techniques explained in Refs. 11 and 12. Currently, the consensus view is that a flow is quiet if the freestream is spatially and temporally uniform with acoustic and convected disturbances (ratio of total pressure rms to total pressure, $p_{\text{rms}}/p_{\text{total}}$) less than 0.1% (Refs. 11–13). Because conditions in the tunnel are all well below this level and approaching that of the signal noise level, the tunnel may be considered quiet in the acoustic sense. With a 5-μm tungsten hot wire, the freestream fluctuation value at the centerline of the tunnel was found to be 0.035% (Ref. 10), which is also very low.

To raise the disturbance level in the test section, 0.5-in.-wide strips of size 80 grit sandpaper (0.025-in. height) were stuck to upper and sidewalls of the tunnel. The weak shock waves generated by the trips passed in front of the model to avoid any possible impingement on the attachment-line boundary layer. These trips were sufficient to produce turbulent boundary layers on the tunnel walls, and this caused the test section to be irradiated with acoustic disturbances. Figure 2 shows that tripping the tunnel walls increases the rms pressure disturbance level of the freestream by a factor of eight. The disturbance was also found to be broadband, as indicated in Fig. 3.

The leading-edge test flow was generated on a circular cylinder swept at 76 deg, with the apex aligned with the freestream direction (Fig. 4). Two models, identical in external geometry, were used: a pressure model for the determination of the surface pressure distribution and a model instrumented with thermocouples for the transition tests. Both had external diameters of 1.6 in. and were 16 in. in length. They were supported from the upper wall of the test section by a wedge-shaped spacer and were swept forward in the centerline

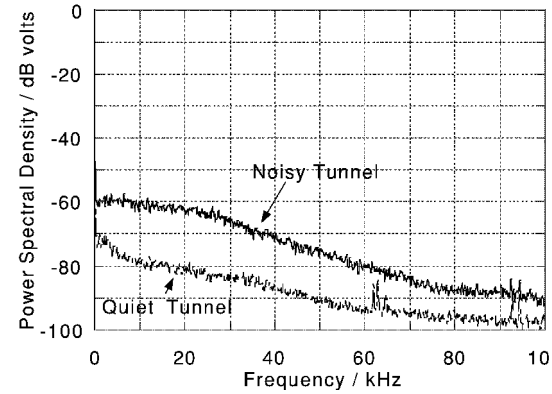

Fig. 3 Effect of tripping wind-tunnel walls on freestream frequency spectra, tunnel centerline 1.0 in. downstream of the nozzle exit; Re_∞ = 3.65 × 10^6/ft.

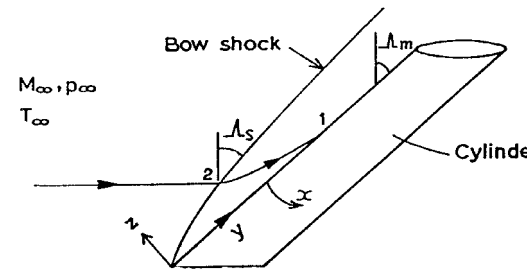

Fig. 4 Semi-infinite circular cylinder in supersonic flow.

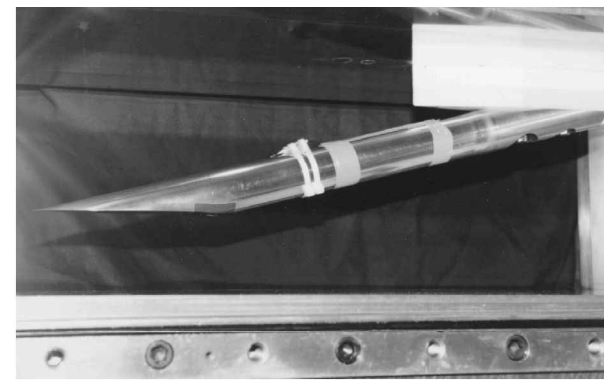

Fig. 5 Thermocouple instrumented model setup for trip-wire testing.

vertical plane, as shown in Fig. 5. This arrangement was chosen to prevent the apex from coming too close to the floor of the tunnel and, thus, to avoid any possible contamination of the attachment-line flow by the tunnel wall boundary layer. The configuration was such that the bow shock from the upstream tip reflected from the upper tunnel wall and impinged on the attachment line, ending the useful test length of the cylinder, at approximately 8 in. from the tip.

The transition model was made of aluminum 6061-T6 and had a wall thickness of approximately 0.125 in. Its surface was highly polished and finished to better than 1×10^{-5} in. rms. Five T-type thermocouples were evenly placed along the attachment line, from 3.7 to 11.7 in. ($2.3 < y/D < 7.3$) from the apex. Flow state in the attachment-line boundary layer was determined with a 2.5-μm-diam, copper-plated, tungsten hot-wire anemometer. The probe was attached to the cylinder surface using two plastic ties, and the height of the wire above the model surface was set at 0.010 in. in the wind-off condition.

To estimate the chordwise velocity gradient, which is required to obtain the local characteristic Reynolds number, chordwise surface pressure information is required. In previous experiments (with the exception of that of Yeoh[14]), the velocity gradient has been obtained by assuming infinite swept conditions and a modified Newtonian (or

similar) pressure distribution around the chord. This was deemed unacceptable for the present study because accurate local Reynolds numbers were required. Because pressure tap orifices are known to cast off disturbances, which can influence boundary-layer transition data, a second model was used for pressure measurements. This had a series of taps placed along the attachment line from 3.7 to 7.7 in. ($2.3 < y/D < 4.8$) from the apex, at 1-in. intervals. At each spanwise location, they extended in the chordwise (normal to the attachment line) direction from −50 to +50 deg, in 10-deg intervals, making a total of 66 pressure-measuring points in all.

Mean Flow Computational Fluid Dynamics (CFD) Calculations

The CFL3D[15] code was used, in inviscid mode, to calculate the mean flow around the cylinder. This provided the viscous-layer edge conditions for subsequent boundary-layer computations using a simplified version of BL3D.[16] The CFL3D grid had a C–H topology consisting of 222, 74, and 102 points in the x, y, and z directions, respectively, and was operated in Euler mode with flux difference splitting. BL3D was run for the adiabatic wall case. The boundary-layer grid was specified, to calculate attachment-line parameters. It did not extend in the chordwise direction and consisted of 52 and 81 points in the y and z directions, respectively.

The characteristic viscous layer Reynolds number at the attachment line is $\bar{R}$ (see Ref. 17) where

$$\bar{R} = V_e \eta_e / \nu_e$$

$$\eta_e = \left[\nu_e \Big/ \left(\frac{\mathrm{d}U_e}{\mathrm{d}x} \right)_{x=0} \right]^{\frac{1}{2}}$$

The resulting $\bar{R}$ distributions at two freestream conditions are shown in Fig. 6. These correspond to the maximum and minimum values obtainable in the tunnel for this model and sweep angle. However, note that this arrangement produces an $\bar{R}$ in excess of 700, which is close to the level expected on projected High Speed Civil Transport aircraft in the cruise. Figure 7 shows the corresponding viscous length scale η and boundary-layer thickness δ along the attachment line. Note that, although the model has a relatively short span, the boundary-layer thickness reaches a near-constant value at all conditions within two cylinder diameters' distance from the tip.

Evaluation of $\bar{R}$ from Surface Pressure Measurements

To evaluate $\bar{R}$, the chordwise distribution of velocity is needed at each spanwise location, and this requires a knowledge of the boundary-layer edge temperature and pressure at the attachment line (p_A and T_A, respectively[18,19]). With the instrumentation available, it was not possible to obtain direct measurements of T_A, and, therefore, it was necessary to obtain T_A from knowledge of the local surface static pressure p_A and shock angle Λ_s.

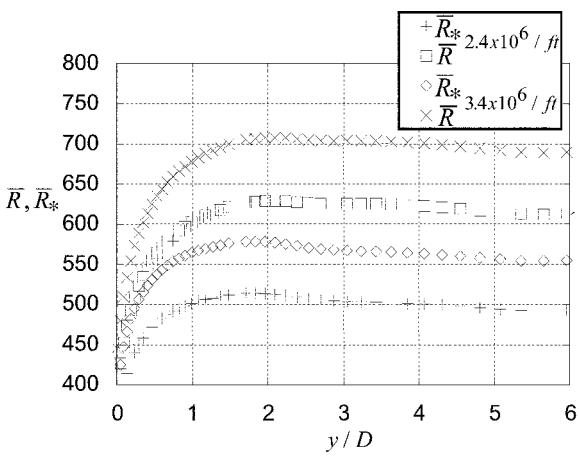

Fig. 6 Theoretical prediction of $\bar{R}$ and $\bar{R}_*$ along the attachment line; $Re_\infty = 2.4 \times 10^6$/ft and 3.4×10^6/ft.

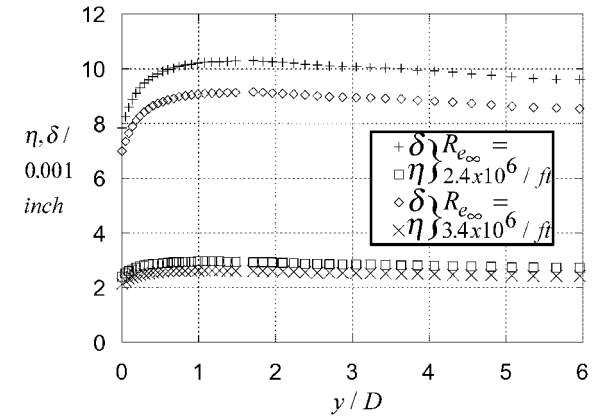

Fig. 7 Predicted variation of η and δ along the 76-deg attachment line.

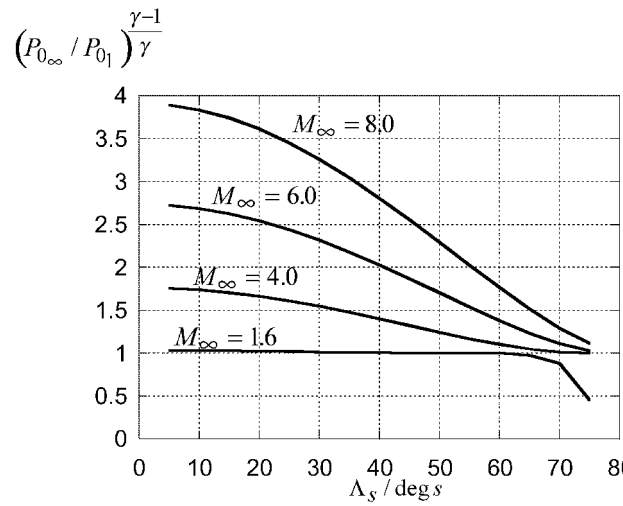

Fig. 8 Effect of M_∞ and Λ_S on the total pressure of the streamlines entering the attachment line from the freestream.

Consider the situation shown in Fig. 4. The streamline that first enters the boundary layer at the point 1 has passed through the bow shock at the point 2. Hence, we may write

$$\frac{p_A}{p_\infty} = \frac{p_A}{p_{0_1}} \frac{p_{0_1}}{p_{0_\infty}} \frac{p_{0_\infty}}{p_\infty}$$

With the incorporation of the oblique shock relations, it follows[18] that

$$\frac{T_A}{T_\infty} = \left[\frac{p_A}{p_\infty} \right]^{(\gamma-1)/\gamma} \left[\frac{(\gamma-1)M_\infty^2 \cos^2 \Lambda_s + 2}{(\gamma+1)M_\infty^2 \cos^2 \Lambda_s} \right]$$

$$\times \left[\frac{2\gamma M_\infty^2 \cos^2 \Lambda_s - (\gamma-1)}{(\gamma+1)} \right]^{1/\gamma}$$

This equation allows the unknown temperature T_A to be obtained from the measured surface static pressure and the shock sweep angle, measured from schlieren photographs. All other flow parameters at the edge of the attachment-line boundary layer follow immediately.[18]

When examining schlieren photographs, it is necessary to estimate where the streamline that impacts the attachment line at a given y location crosses the bow shock. In general, this is not known. Therefore, an analysis was undertaken to determine the sensitivity of T_A to the shock angle Λ_s. Now

$$\left(\frac{p_{0_\infty}}{p_{0_1}} \right)^{(\gamma-1)/\gamma} = \frac{(T_A/T_\infty)}{(p_A/p_\infty)^{(\gamma-1)/\gamma}}$$

Therefore, for fixed freestream conditions and known p_A, parameter T_A depends on p_{0_∞}/p_{0_1}. This ratio is plotted in Fig. 8 as a function of freestream Mach number and shock angle. For Mach 1.6, p_{0_∞}/p_{0_1}

is approximately constant up to a value of Λ_s of 65 deg. Because schlieren visualization showed that the bow shock was still highly curved near the apex of the cylinder[10] and because the streamline of interest must pass through the shock close to the apex, Λ_s will be below this value. Consequently, the value of Λ_s has very little effect on the results. If the freestream Mach number was higher, the choice of Λ_s would become much more important and some form of flow visualization would be required to establish the exact point at which the streamline of interest crossed the bow shock.

The chordwise velocity was shown by Poll[19] to be given by

$$U_e = a_A\left\{ 2/(\gamma-1)\left[1-(p_e/p_A)^{(\gamma-1)/\gamma}\right]\right\}^{\frac{1}{2}}$$

Although strictly valid for an infinite swept flow, provided that V_∞ does not vary significantly with θ, the relation holds for a finite length model. It was found that by fitting polynomials to the chordwise velocity distribution, accurate estimates of the velocity gradient term could be obtained.[10] In this case, fifth-order polynomials were fitted to the velocity distributions obtained at each spanwise location using a least-squares technique.

Surface Pressure Results

The three parameters of interest, p_{0_∞}, p_∞, and $p_e - p_\infty$, were acquired for freestream unit Reynolds numbers 2.4×10^6/ft to $Re_\infty = 3.4 \times 10^6$/ft in 0.2×10^6/ft intervals. They were recorded via an A/D converter running at 50 Hz for 80 s, giving a total of 4000 samples over three channels. These were averaged to produce mean pressures and a mean value of C_p for each port.[10] As expected, there was no variation in the C_p distribution due to changes in the freestream unit Reynolds number, and Fig. 9 shows the complete distribution over the cylinder. The experimentally obtained C_p distribution along the attachment line is compared with the computational fluid dynamics (CFD) solution in Fig. 10. The two are similar and both are approaching the infinite swept value of 0.061 at large y/D. Figure 11 shows the experimentally obtained $\bar{R}$ distribution ($\bar{R}$ accuracy $= \pm 5\%$) for freestream unit Reynolds numbers of 2.4×10^6/ft and 3.4×10^6/ft. Compared to the CFD results, the experimental values are higher by about 10%. For the purposes of data reduction, the experimental values have been used.

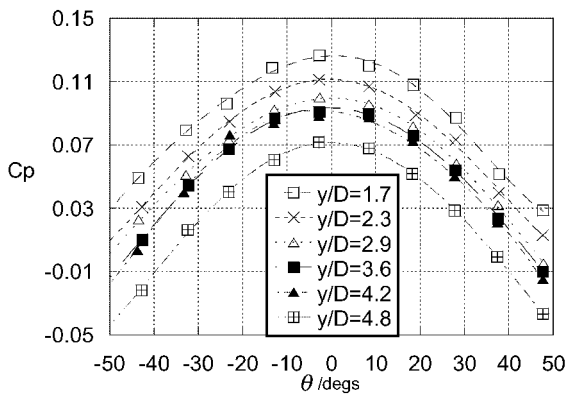

Fig. 9 Experimental surface C_p distribution on the swept cylinder.

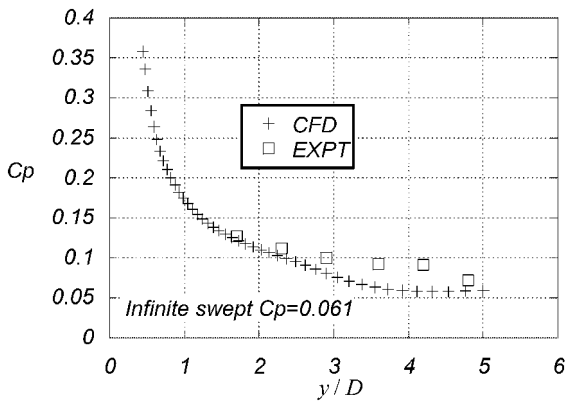

Fig. 10 Comparison of the experimental and theoretical C_p distributions along the attachment line.

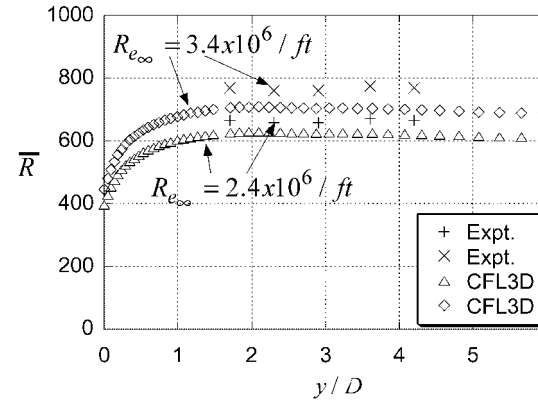

Fig. 11 Experimental and theoretical $\bar{R}$ distribution along the attachment line at $Re_\infty = 2.4 \times 10^6$/ft and 3.4×10^6/ft.

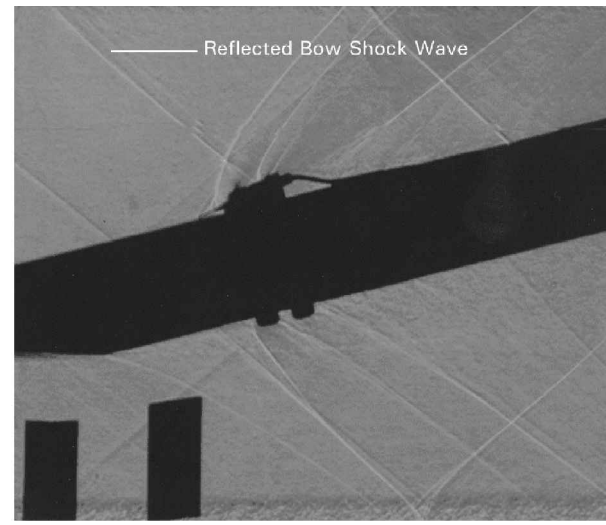

Fig. 12 Reflected bow shock hitting the rear of the hot-wire probe body at $y/D = 5.6$; $Re_\infty = 2.4 \times 10^6$/ft; distance between tapes is approximately 1 in.

Surface Temperature Results

Thermocouple response to changes in tunnel freestream total temperature was rapid, and the model reached thermal equilibrium, approximately the adiabatic wall condition, in a few minutes. The temperature along the attachment line was almost uniform, with the maximum difference between any two thermocouples being of the order 1°F. Based on a wall temperature of 0°F (−17.8°C) and a stagnation temperature of 20°F (−6.7°C), the recovery factor for the laminar flow was estimated to be 0.84.

Flow Visualization

Schlieren visualization showed that the bow shock was attached at the tip and was curved. The overall shape was in reasonable agreement with the CFL3D solution. At the tip, the shock wave angle was 50 deg, reducing to 43 deg, whereas the CFL3D solution gave 45 deg reducing to 40 deg. Figure 12 shows the reflected bow shock hitting the rear of a hot-wire probe at a spanwise distance of 9 in. ($y/D = 5.6$) from the tip. There were Mach waves emanating from various joints of the wind-tunnel walls. However, they are located near to the walls, they do not span the tunnel, and none impinged on the transition test surface.

Oil flow visualization was also used to gain an understanding of the overall flow pattern.[10] The line of flow separation was clearly visible at around 90 deg upstream of the incident shock wave, moving up to 70 deg downstream of the shock impingement position. This provided additional evidence that the attachment-line boundary layer was free from external disturbances.

Transition and Trip-Wire Results

With the hot-wire probe positioned just in front of the reflected bow shock wave, it was found that, for adiabatic wall condition, the clean (no trip) cylinder had a laminar and stable, attachment-line flow up to the highest Reynolds number attainable, that is, $\bar{R}$ equals approximately 790 at a distance of $s/\eta = 3300$ from the apex.

Trip wires were then placed on the model. During these tests, the hot wire was always positioned at 8 in. from the apex to maximize spanwise test length, and trips (from 0.001- to 0.025-in. diam) were placed at various distances from the tip (from 3.88 to 7.5 in.). A weak pressure gradient along the cylinder is evident between the location of the trip wires ($2.4 < y/D < 4.7$) and the hot wire ($y/D = 5.0$) (Fig. 10).

The placement of trip wires at various distances from the cylinder tip over the Reynolds number range permitted the observation of laminar, intermittent, and fully turbulent flows. Turbulent hot-wire signals, with the characteristic power spectrum, were obtained with large trip wires, and these differed considerably from the laminar, untripped signals under the same condition. Focused schlieren flow visualization of the attachment-line boundary layer was also attempted, and the results are given in Fig. 13. This provided an estimate of the laminar and turbulent boundary-layer thicknesses of 0.007 and 0.025 in., respectively. The laminar result is quite close to the BL3D prediction of 0.009 in.

With a 0.009-in. trip placed at 6.5 in. from the tip and the hot wire at 8.0 in. from the tip, laminar, intermittent, and fully turbulent flows were observed as the Reynolds number was increased (Fig. 14). The appearance of turbulent flow was accompanied by a rise in the equilibrium wall temperature, and the recovery factor rose from 0.86 to 0.88. An intermittency of 5% (appearance of bursts) in the hot-wire signal was used as a threshold for the definition of transition onset.

The tripped flow results are shown in Figs. 15 and 16. Figure 15 shows that the trip Reynolds number for this Mach number appears to be just below 1900. This is close to the value of 2000 found for

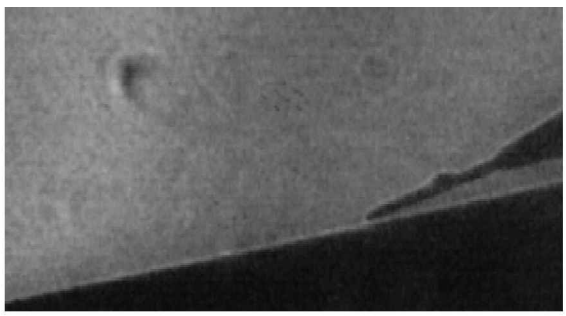

Wind off

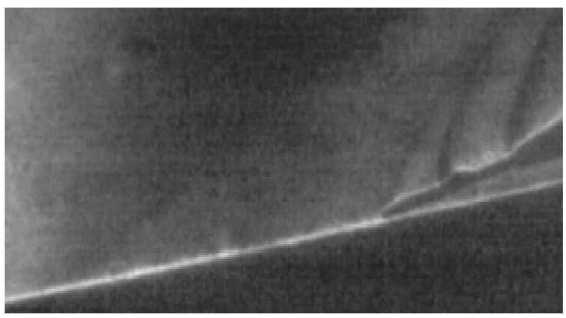

Laminar flow. No trip, $\bar{R}$=790.

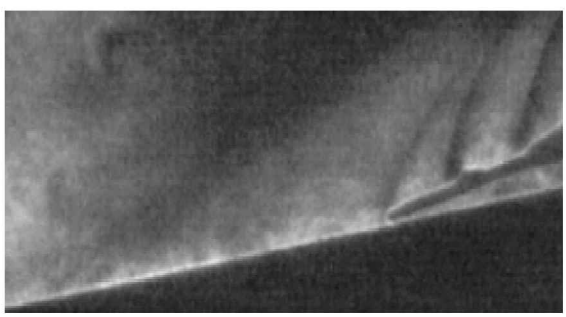

Turbulent flow. 0.025 inch trip wire at y/D = 4.2, $\bar{R}$=790.

Fig. 13 Focused schlieren photographs of the attachment-line boundary layer, showing the difference between laminar and turbulent cases; hot wire at y/D = 5.0.

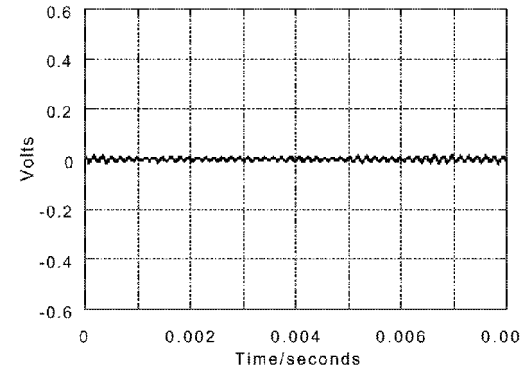

Laminar flow: $\bar{R}$ = 596 ($\bar{R}_*$ = 480), Re_k = 1896, k/η = 3.10, s/η = 517, r = 0.864. rms = 7 mV

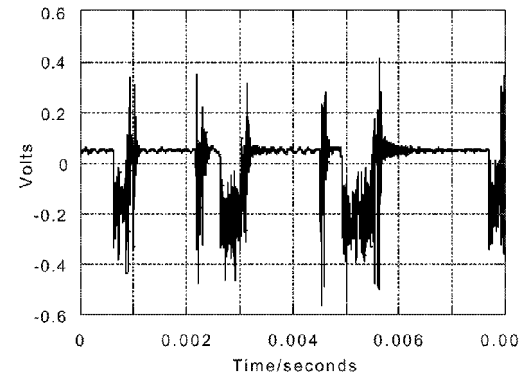

Intermittent flow (intermittency ≈ 40%): $\bar{R}$ = 657 ($\bar{R}_*$ = 529), Re_k = 2292, k/η = 3.42, s/η = 570, r = 0.868. rms = 121 mV

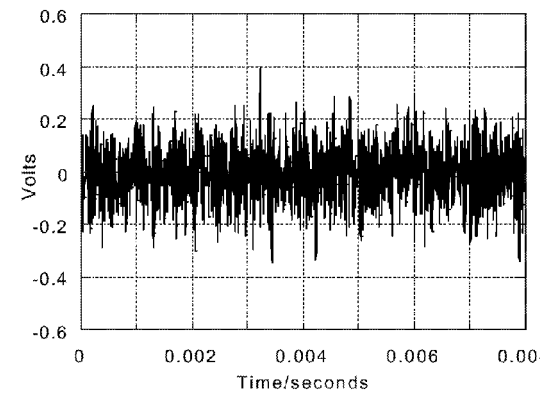

Turbulent flow (intermittency ≈ 100%): $\bar{R}$ = 700 ($\bar{R}_*$ = 560), Re_k = 2636, k/η = 3.63, s/η = 605, r = 0.880. rms = 98 mV

Fig. 14 Observation of laminar, intermittent, and turbulent flow with a 0.009-in. trip wire at y = 6.5 in. (y/D = 4.1).

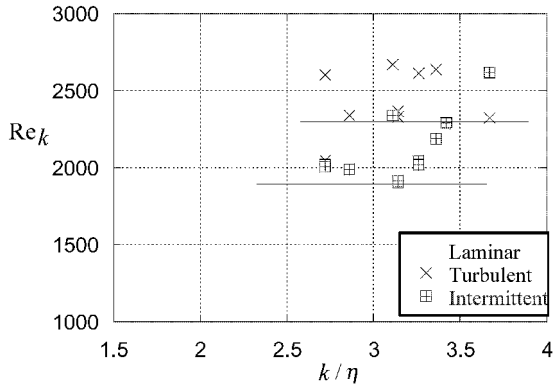

Fig. 15 Local trip-wire Reynolds number at transition onset as a function of nondimensional trip height.

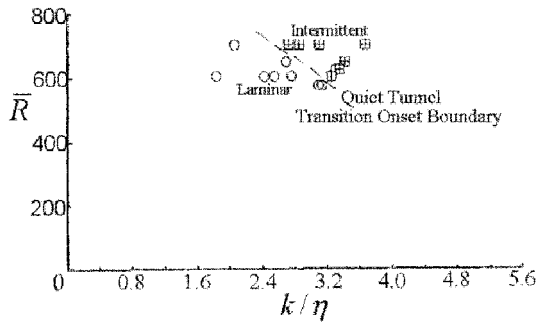

Fig. 16 Transition onset boundary in the Mach 1.6 low-disturbance wind tunnel.

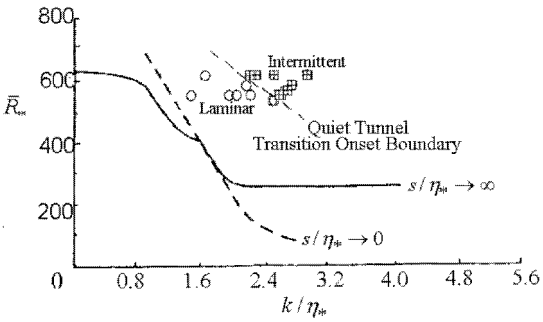

Fig. 17 Comparison between reference temperature transformed data and the incompressible results of Poll.[22]

transition onset on a flat plate at a Mach number of 2.0 with an adiabatic wall, as reported in Ref. 20. Figure 16 gives the variation of $\bar{R}$ with k/η (Ref. 21) for transition onset.

In Ref. 17, Poll suggested that in the situation where transition is induced by a very large trip wire ($k/\eta \to \infty$), the onset Reynolds number in compressible flow can be transformed to the transition onset value for incompressible flow by the use of the reference temperature T_*, that is, by replacing $\bar{R}$ with $\bar{R}_*$ where

$$\bar{R}_* = V_e \eta_* / \nu_*$$

The transition behavior of the incompressible attachment line in the presence of small and large trip wires is well known and described in detail in Ref. 22. Figure 17 gives the skeleton of the incompressible results, together with the present data, suitably transformed. It is clear that, although the reference temperature transformation does move the compressible results toward the incompressible line, the data are not completely reduced to the equivalent incompressible values. This difference may be due to the low-disturbance environment of the tunnel because increased disturbance levels in the presence of trips can have a marked effect on the transition process. This has been observed by Creel and Beckwith[2] and Creel et al.[3]

To test this hypothesis, a simple experiment was carried out. When the tunnel was clean and a 0.005-in.-diam trip wire was placed on the cylinder at 4 in. from the apex, the recorded signal at $y = 8$ in. was laminar ($\bar{R} = 790$ and $k/\eta = 2.04$). With the tunnel wall boundary-layer tripped and the freestream disturbance level increased (Fig. 3), intermittent bursts were observed at the same condition. This suggests that increased levels of tunnel disturbances do reduce the Reynolds numbers for transition to turbulence in the presence of a trip wire.

Summary

A procedure for the estimation of the attachment-line Reynolds number $\bar{R}$ from surface pressure measurements and schlieren visualization has been outlined. Theoretical values of $\bar{R}$ have been shown to be in reasonable agreement with those obtained experimentally. It has been shown that in the low-disturbance environment of the NASA Ames Research Center quiet tunnel and for near adiabatic wall conditions, the attachment-line boundary layer remains laminar up to the largest obtainable $\bar{R}$, that is, 790 at an s/η of 3300. It has also been shown that attachment-line boundary-layer transition in the presence of two-dimensional trips is a function of both trip diameter and wind-tunnel disturbance level. An approximate transition onset boundary has been established.

Acknowledgments

The assistance of Venkit Iyer (High Technology Corporation, Hampton, Virginia) is greatly appreciated for providing the CFL3D and BL3D computational grids and computational fluid dynamics consultation. James Heineck (NASA Ames Research Center) is also acknowledged for his assistance with the schlieren photographic technique.

References

[1] Arnal, D., Vignau, F., and Juillen, J. C., "Boundary Layer Tripping in Supersonic Flow," *Laminar–Turbulent Transition*, edited by D. Arnal and R. Michel, Springer-Verlag, Berlin, 1989.

[2] Creel, T. R., and Beckwith, I. E., "Effects of Wind-Tunnel Noise on Swept Cylinder Transition at Mach 3.5," AIAA Paper 86-1085, May 1986.

[3] Creel, T. R., Beckwith, I. E., and Chen, F. J., "Transition on Swept Leading Edges at Mach 3.5," *Journal of Aircraft*, Vol. 25, No. 10, 1987, pp. 710–717.

[4] Da Costa, J. L., de la Chevalerie, D. A., and de Roquefort, T. A., "Leading Edge Transition by Contamination in Hypersonic Flow," CP-438, AGARD, 1988.

[5] Holden, M., and Kolly, J., "Attachment Line Transition Studies on Swept Leading Edges at Mach Numbers from 10 to 12," AIAA Paper 95-2279, June 1995.

[6] Murakami, A., Stanewsky, E., and Krogmann, P., "Boundary-Layer Transition on Swept Cylinders at Hypersonic Speeds," *AIAA Journal*, Vol. 34, No. 4, 1996, pp. 649–654.

[7] Skuratov, A. S., and Federov, A. V., "Supersonic Boundary Layer Transition Induced by Roughness on the Attachment Line of a Yawed Cylinder," *Izvestiya Akademii Nauk SSSR, Mekhanika Zhidkosti i Gaza*, Vol. 6, 1990, pp. 28–35.

[8] Benard, E., Gaillard, L., and de Roquefort, T. A., "Influence of Roughness on Attachment Line Boundary Layer Transition in Hypersonic Flow," *Experiments in Fluids*, Vol. 22, 1997, pp. 286–291.

[9] Coleman, C. P., Poll, D. I. A., Laub, J. A., and Wolf, S. W. D., "Leading-Edge Transition on a 76-Degree Swept Cylinder at Mach 1.6," AIAA Paper 96-2082, June 1996.

[10] Coleman, C. P., "Boundary Layer Transition in the Leading Edge Region of a Swept Cylinder in High Speed Flow," NASA TM-1998-112224, March 1998.

[11] Wolf, S. W. D., Laub, J. A., and King, L. S., "Flow Characteristics of the NASA-Ames Laminar Flow Supersonic Wind Tunnel for Mach 1.6 Operation," AIAA Paper 94-2502, June 1994.

[12] Wolf, S. W. D., and Laub, J. A., "Low-Disturbance Flow Characteristics of the NASA-Ames Laminar Flow Supersonic Wind Tunnel," AIAA Paper 96-2189, June 1996.

[13] Laufer, J., "Factors Affecting Transition Reynolds Numbers on Models in Supersonic Wind Tunnels," *Journal of the Aeronautical Sciences*, Vol. 21, No. 7, 1954, pp. 497, 498.

[14] Yeoh, K. B., "Transition Along the Attachment Line of a Swept Cylinder in Supersonic Flow," M.S. Thesis, College of Aeronautics, Cranfield Univ., Cranfield, England, U.K., Sept. 1980.

[15]Thomas, J., Krist, S., and Anderson, W., "Navier–Stokes Computations of Vortical Flows," *AIAA Journal*, Vol. 28, No. 2, 1990, pp. 205–212.

[16]Iyer, V., "Three-Dimensional Boundary-Layer Program (BL3D) for Swept Subsonic or Supersonic Wings with Application to Laminar Flow Control," NASA CR 4531, 1993.

[17]Poll, D. I. A., "The Development of Intermittent Turbulence on the Swept Attachment Line Including the Effects of Compressibility," *Aeronautical Quarterly*, Vol. 34, Feb. 1983, pp. 1–23.

[18]Poll, D. I. A., "Boundary Layer Transition by Attachment-Line Contamination in a Compressible Flow with Heat Transfer," Dept. of Aeronautical Engineering, Rept. 8911, Univ. of Manchester, Manchester, England, U.K., July 1989.

[19]Poll, D. I. A., "3-D Transition to Turbulence by Contamination. Part II—Accurate Determination of the Attachment-Line Chordwise Velocity Gradient," Dept. of Aeronautical Engineering Rept. 9311, Univ. of Manchester, Manchester, England, U.K., March 1993.

[20]Gibbings, J. C., "On Boundary Layer Transition Wires," Aeronautical Research Council, CP-462, 1959.

[21]Poll, D. I. A., "Some Aspects of the Flow Near a Swept Attachment Line with Particular Reference to Boundary Layer Transition," Ph.D. Dissertation, College of Aeronautics, Cranfield Inst. of Technology, Cranfield, England, U.K., June 1978.

[22]Poll, D. I. A., "Transition in the Infinite Swept Attachment Line Boundary Layer," *Aeronautical Quarterly*, Vol. 30, Nov. 1979, pp. 607–629.

M. Samimy
Associate Editor